doi: 10.56761/EFRE2022.S6-P-021101

2D kinetic modeling of plasma jet in external magnetic field

D.L. Shmelev[1,4,], I.V. Uimanov[1], S.A. Barengolts[2], M.M. Tsventoukh[3]*

[1]*Institute of Electrophysics UB RAS, Ekaterinburg, Russia*
[2]*Prokhorov General Physics Institute RAS, Moscow, Russia*
[3]*Lebedev Physical Institute RAS, Moscow, Russia*
[4]*Ural Federal University, Ekaterinburg, Russia*
[*]*shmelev@iep.uran.ru*

Abstract. This article presents some preliminary results of a 2D PIC MC kinetic simulation of the effect of an external axial magnetic field (AMF) on a plasma jet emanating from a vacuum arc cathode spot. It is shown that a strong AMF leads to compression of the plasma jet with the formation of a complex multi-stream ion flow in the central region of the plasma jet and the appearance of a positive potential hump in the peripheral layers of the plasma jet. In addition, it is shown that the density of the ion current from the plasma to the cathode increases with increasing AMF.
Keywords: vacuum arc, plasma jet, cathode spot, magnetic field, numeric simulation.

1. Introduction

The study of the behavior of plasma jets flowing from the cathode spot of a vacuum arc in an external axial magnetic field (AMF) is supported primarily by the widespread use of vacuum arc interrupters with AMF [1]. In addition, the effect of AMF on the increase in the average ion charge in vacuum-arc ion sources is of interest [2]. Recently, interest has arisen in the behavior of cathode spots on the divertor surface in tokamaks, where the magnetic field is almost perpendicular to the surface [3]. Previously, various magnetohydrodynamic and hybrid quasi-neutral approximations were used to simulate a plasma jet with AMF [4–7]. In this paper, we present the first results of modeling the cathode spot plasma jet with AMF using the kinetic non-quasi-neutral approximation.

2. Brief model description

The kinetic model used in this work is a development of the kinetic models used earlier, for example, in [8, 9]. The model is a two-dimensional and axisymmetric model. The computational domain is a rectangle with dimensions of 22×60 μm. Ions and electrons enter the computational domain through a cathode spot with a radius of 5 μm. In this model, the processes of evaporation, emission, and ionization occurring in a real cathode spot are not considered. Here, only the motion of particles in a self-consistent field by the particle-in-cell (PIC) method and the Coulomb scattering of electrons and ions by the Monte Carlo (MC) method are considered. The cathode spot here is only a source of current and a supersonic ion flux, which in reality is formed at a distance of several microns from the normal cathode spot. In this model, the flow of doubly charged aluminum ions is set, having an average velocity of $2.6 \cdot 10^6$ cm/s. Those, our "cathode spot" is presumably a few microns higher than the actual cathode spot.

It is assumed that the cathode spot in this model has an infinite emissivity. The current density distribution in the spot is calculated according to the Child-Langmuir law from the voltage drop at the first step of the computational grid. In this case, the current is distributed unevenly along the radius with a maximum located at the border of the cathode spot. The total spot current is 1 A. The specific erosion of ions is 7.5 μg/C. This value is two times less than the normal erosion of aluminum. With the chosen parameters, the electron density in the region of the cathode spot is about 10^{17} cm^{-3}. The temperatures for particles entering the computational domain are set at 4 eV for electrons and 1 eV for ions.

The boundaries of the computational domain (except for the cathode spot and the axis of symmetry) are passive ideally absorbing boundaries. The lower boundary (cathode) (see for example Fig.1) has zero electrical potential. The potential at the upper boundary (anode) is set in the

course of solving the problem in such a way as to ensure the total arc current equal to 1 A. In the quasi-stationary mode, the anode potential is on the order of several volts. The external axial magnetic field (AMF) is set uniformly distributed over the entire computational domain.

3. Results and discussion

Examples of distributions of various plasma parameters for a steady quasi-stationary flow for two AMF values are shown in Fig.1–5. It can be seen that as the AMF increases, the plasma jet (Fig.1, Fig.2) and the current channel (Fig.3, Fig.4) shrink. Although it would be more correct to say that the AMF prevents the plasma jet from expanding under the pressure gradient.

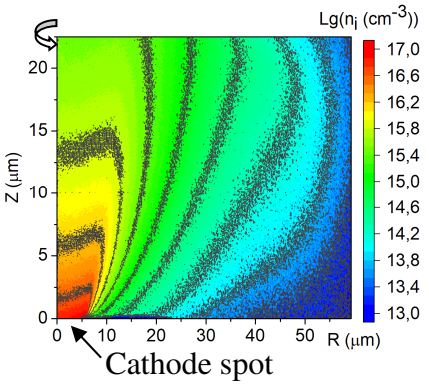

Fig.1. Ion density distribution. AMF-1 T.

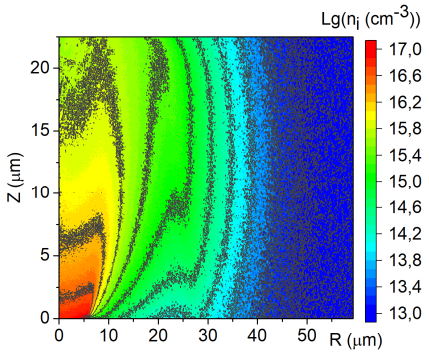

Fig.2. Ion density distribution. AMF-2.5 T.

Oscillations are noticeable in the current density distribution near the axis (Fig.3). These oscillations are a consequence of the development of ion-acoustic instability. This instability develops relatively slowly and does not lead to plasma decay.

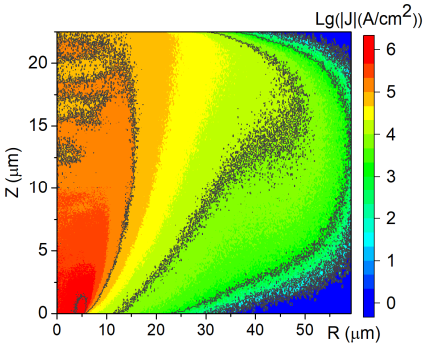

Fig.3. Electron current density distribution. AMF-1 T.

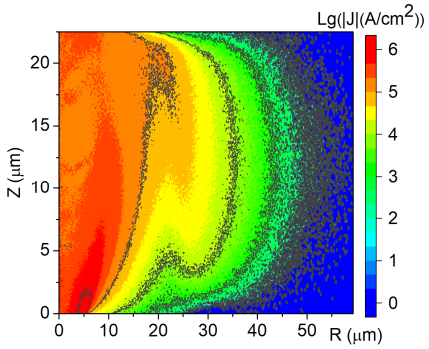

Fig.4. Electron current distribution. AMF-2.5 T.

It should be recalled that the direct effect of AMF on ion motion under these conditions is negligibly small. AMF has a strong effect on electrons. The polarization electric field (Hall electric field) formed during compression of the electronic subsystem causes the ionic subsystem to contract as well. Near the electrodes, the Hall field is neutralized. This results in a constriction of the electron current in the vicinity of the electrodes (Fig.4). Without AMF, electrons predominate in the outer low-dense layers of the plasma jet and an uncompensated negative space charge is formed. When the plasma jet is compressed under the action of AMF, ions predominate in the outer layers and a positive space charge is formed, resulting in a potential hump (Fig.5–8). The height of this potential hump can significantly exceed the voltage drop across the interelectrode gap.

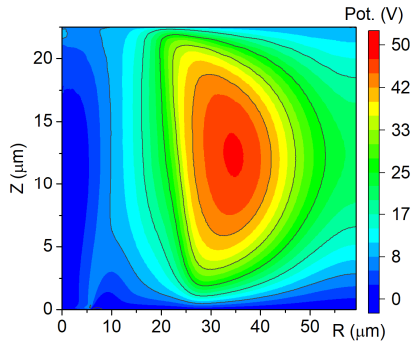

Fig.5. Electric potential distribution. AMF – 2.5 T.

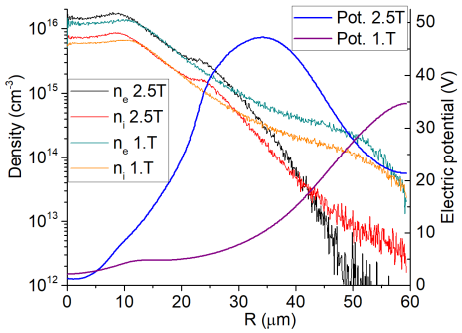

Fig.6. Electric potential, electron, and ion densities along R at a distance 12 μm from cathode.

As follows from Fig.6, the plasma jet can be divided into a central part, where the plasma density relatively weakly depends on R, and an extensive “halo”, where the plasma density decreases exponentially in the R direction. It can be seen that there is no clearly defined boundary of the plasma jet. Note that the electron current density in the “halo” region also decreases with increasing R, but much more slowly than the electron density.

Kinetic methods make it possible to “see” all the details of the flow. Examples of phase portraits of electrons and ions are shown in Fig.7, Fig.8. AMF first reduces electron expansion. As a result, an electric field arises that slows down the expansion of ions (clearly visible in Fig.7a). With a further increase in AMF, the ion velocity in the transverse direction drops below the ion-acoustic one and something like a shock wave appears (clearly seen in Fig.8a). It can be seen that some of the ions are reflected from the potential hump and returned back to the region of the jet core. A smaller part of the ions overcome the potential barrier and fall onto the boundaries of the calculated domain. It can be seen that in a plasma jet in a strong AMF, a complex multistream flow can arise, which cannot be reproduced in the usual MHD approximation. However, the hybrid approximation [6] reproduces such behavior.

Fig.9 shows the distributions of ion and electron current densities coming from the plasma to the cathode. It can be seen that, near the cathode spot, the density of the backward electron current exceeds the density of the ion current from the plasma to the cathode by more than two orders of magnitude. The reverse electron current rapidly decreases with increasing radius, and the ion current from the plasma to the cathode dominates in the outer regions. With an increase in AMF, the region of dominance of the backward electron current decreases. In this case, there is no noticeable increase in the maximum of the backward electron current. In the case of ions, the maximum value of the ion current density to the cathode increases significantly with increasing AMF.

The average kinetic energies of electrons and ions incident on the cathode are shown in Fig.10. It can be seen that the average ion kinetic energies significantly exceed those for electrons, which is due to the large average velocities of ions entering the computational domain, which are characteristic of a vacuum arc. As the AMF increases, the energies of both ions and electrons increase, and the plasma heats up. In the outer layers of the jet, the electron temperature reaches several tens of electron volts, but the particle density in these regions is relatively low.

Recall that the ion current from the plasma to the cathode can be the cause of the reverse motion of cathode spots of the first type in a transverse magnetic field [10]. Cathode spots of the first type are rapidly moving cathode spots on a cathode whose surface is contaminated with dielectric films. It is assumed that the ion current can lead to film charging followed by breakdown and ignition of a new cathode spot.

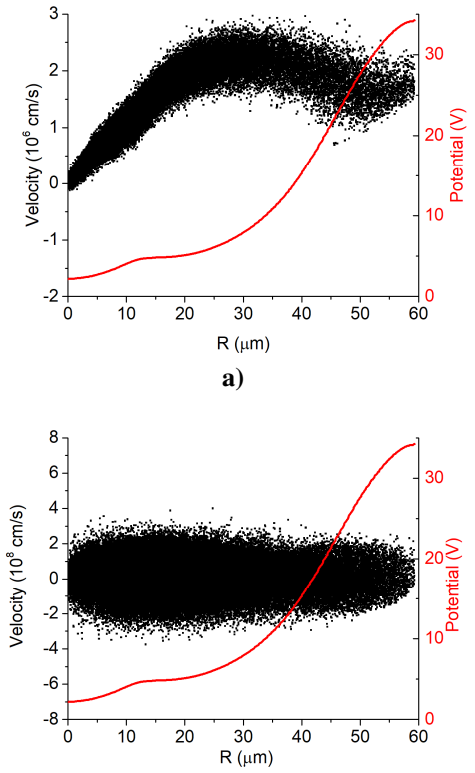

Fig.7. Ion (a) and electron (b) phase portrait and electric potential (red curve) along R direction at distance 15 μm from cathode. AMF – 1 T.

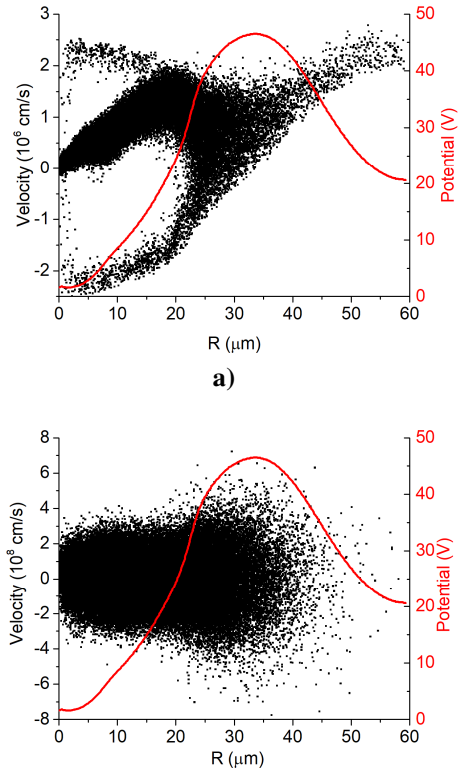

Fig.8. Ion (a) and electron (b) phase portrait and electric potential (red curve) along R direction at distance 15 μm from cathode. AMF – 2.5 T.

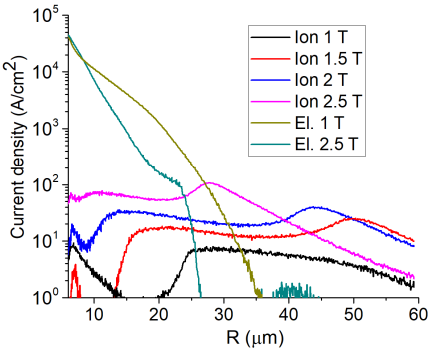

Fig.9. Densities of backward electron and ion current from plasma to cathode at various AMF.

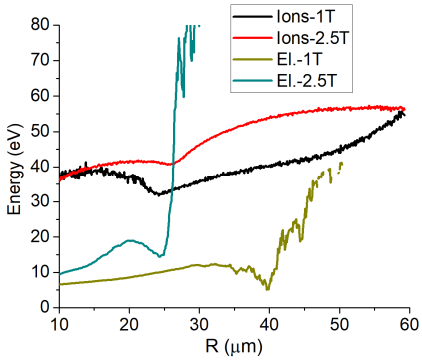

Fig.10. Average energy of electron ad ion falling from plasma to cathode for different AMF.

Within the framework of the approximation described in this work, we cannot simulate the effect of a transverse magnetic field on the plasma jet of the cathode spot due to geometric limitations. However, let us assume for a second that the behavior of the plasma jet on the side of the maximum transverse magnetic field qualitatively coincides with that in the presence of AMF. Then we obtain an increase in the ion current with an increase in the magnetic field, which, according to [10], means an increase in the probability of the appearance of a new cathode spot in the direction of the maximum transverse magnetic field, which coincides with the anti-ampere

direction. Thus, the results of our simulation provide additional arguments in favor of the model [10].

4. Conclusion

Some preliminary results of two-dimensional kinetic modeling by the PIC MC method of the action of an external AMF on a plasma jet flowing from the cathode spot of a vacuum arc are presented. It is shown that a strong AMF leads to compression of the plasma jet with the formation of a complex multi-stream ion flow in the central region of the plasma jet and the appearance of a positive potential hump in the peripheral layers of the plasma jet. It is shown that with increasing AMF, the magnitude of the potential hump and the temperature of electrons in the outer layers of the plasma jet increase. In addition, it is shown that the maximum density of the ion current from the plasma to the cathode increases with increasing AMF.

Acknowledgements

The work was supported by the Russian Science Foundation (Grants No 20-19-00323).

5. References

[1] Schade E., *IEEE Trans. Plasma Sci.*, **33**(5), 1564, 2005; doi: 10.1109/TPS.2005.856530
[2] Bugaev A.S., Vizir A.V., Gushenets V.I., et al., *Russ. Phys. J.*, **60**(8), 1392, 2017; doi: 10.1007/s11182-017-1227-z
[3] Hwangbo D., Kajita S., Barengolts S. A., et al., *Contr. Plasma Phys.*, **58**(6–8), 608, 2018; doi: 10.1002/ctpp.201700157
[4] Keidar M., Beilis I., Boxman R.L., Goldsmith S., *J. Phys. D: Appl. Phys.*, **29**(7), 1973, 1996; doi: 10.1088/0022-3727/29/7/034
[5] Shmelev D.L., *Proc. 19th Int. Symp. on Discharges and Electrical Insulation in Vacuum (ISDEIV)*, Xi'an, China, 218, 2000; doi: 10.1109/DEIV.2000.877289
[6] Shmelev D.L., Uimanov V.I., Wang L., *Proc. 4th Int. Conf. on Electric Power Equipment-Switching Technology (ICEPE-ST)*, Xi'an, China, 642, 2017; doi: 10.1109/ICEPE-ST.2017.8188929
[7] Wang L., Zhang X., Deng J., Yang Z., Jia S., *IEEE Trans. Plasma Sci.*, **47**(8), 3496, 2019; doi: 10.1109/TPS.2019.2899659
[8] Shmelev D.L., Uimanov I.V., Barengolts S.A., Tsventoukh M.M., *Proc. 29th Int. Symp. on Discharges and Electrical Insulation in Vacuum (ISDEIV)*, Padova, Italy, 268, 2021; doi: 10.1109/ISDEIV46977.2021.9586863
[9] Shmelev D.L., Barengolts S.A., Tsventoukh M.M., *Plasma Sources Sci. Techn.*, **23**(6), 062004, 2014; doi: 10.1088/0963-0252/23/6/06200
[10] Tsventoukh M.M., Barengolts S.A., Mesyats V.G., Shmelev D.L., *Phys. Lett.*, **39**, 933, 2013; doi: 10.1134/S1063785013110138